A Fully Mechanical Realization of PID Controller

Jiaze Cai

Texas A&M University, State of Texas, United States

Abstract. PID controller is one of the most widely used control elements in the industry. Over history, people have implemented the PID controller mechanically with pneumatical components, electronically in circuits, or digitally using DSP. However, the pure mechanical realization of PID controllers is rarely studied. This paper presents an analog PID controller based on mechanical computation components, including a mechanical integrator, a mechanical differentiator, mechanical constant multipliers, and a mechanical adder. In this work, those parts are studied respectively with CAE modeling and mathematical derivation. A novel design of mechanical differentiator is also introduced to conduct the calculation of the differential part on the PID controller. This work explores the theoretical possibility of a new form of PID controller realization, that is, applying the method of mechanical analog computation to the implementation of a PID controller.

Keywords: PID controller, Analog computer, Mechanical differentiator, Mechanical integrator，Mechanical PID realization.

1. Introduction

1.1 PID controller background:

The proportional-integral-derivative (PID) controller is one of the most important controllers in various industries owing to its simplicity and robustness adequate for most real-world applications. In history, the realization of PID controllers has evolved through the stages of mechanical (or pneumatical), electrical, and digital [1]. Both the mechanical and electrical PID controllers are considered analog controllers, while the digital controllers are discrete controllers. Analog PID controllers are generally realized by constructing physical mechanisms, including pneumatics, thermo-mechanics, electronic circuit, etc., to obtain desired outputs [2]–[4]. In contrast, digital PID controllers are implemented using discrete computer algorithms that calculate the controller output digitally in a microprocessor [5].

1.2 Analog computer background:

Instead of obtaining output from analog mechanisms or calculating output digitally, it is also possible to create an analog PID controller with analog calculation, which can be implemented with an analog computer. The analog computer capable of solving linear differential equations was first introduced by Sir William Thomson (Lord Kelvin) in 1876, followed by his brother Professor James Thomson's invention of the ball-and-disk integrator [6], [7]. The mechanical analog computer calculates the solution of differential equations by feeding the output from series integrations back to the input. The latter mechanical analog computer follows a similar structure to Lord Kelvin's design. One of the notable mechanical analog computers is the differential analyzer built by V. Bush at MIT in 1931 [8], [9]. In this design, Gonnella-wheel-and-disk integrators with torque amplifiers were implemented, which improves the accuracy of calculation [8]. The completion of the differential analyzer provides a new mean to solve complex differential equations for scientists and engineers, which stimulates a surge in building mechanical differential analyzer in universities around the world [9]. With the invention of operational amplifiers, electronic analog computers were built in the 1940s in a similar pattern that Lord Kelvin introduced in 1876 [10]. Note that electronic circuits with resistors, capacitors, and inductors (RLC circuits) can also be used to simulate dynamic systems or to solve differential equations via electrical-mechanical analogies [11]. Owing to its better operationality and higher accuracy, the amplifier-based electronic analog computer was the most widely used [12]. One of the earliest applications of electronic analog computers was on the guidance

system of the A-4 rocket during World War II, which was then generalized to a universal analog computer [13].

1.3 Connection with Analog computer:

As mentioned by Lundberg, "the history of control is entwined with the history of analog computing. Many of the tools, technologies, and theories of control were enabled by, or are directly descended from, mechanical and electronic analog computers [14]." The early analog computers were only used for control system simulation and analysis [15], [16]. Regarding the electric analog PID realization, the operational amplifier circuits are very similar to the circuits used in analog computers [4], [10], [17]. Specifically, components such as adders and integrators are generally interchangeable in both applications [4], [10], [17]. The similarity between electrical analog computation and electrical analog PID controller suggests the possibility of mechanical realization of PID controller using components from mechanical analog computers.

1.4 My work:

Borrowing the idea of mechanical analog computation, this work first introduces a mechanical analog PID controller that calculates the controller output mechanically. The calculated output can then be converted to the application-preferred form. The mechanical PID controller is composed of a mechanical integrator, a novel mechanical differentiator, mechanical constant multipliers, and an adder that sums the output from each component.

2. Methods

Each of the major components of the mechanical PID controller is studied using CAE modeling software and is shown in section 3. The mathematical derivation for each component is also provided in this work. An ideal condition is considered in the mathematical model for simplicity: (1) each part is assumed to be rigid; (2) unwanted friction and mass of parts are assumed to be insignificant; and (3) the dynamic effects of each part are ignored. Thus, there is no delay between input and output from assumptions.

3. Results and Discussion

3.1 PID Schematic

The design of a PID controller contains the fabrication of an integrator, differentiator, and constant multiplier as shown in the schematics (Fig. 1). The input f(t) is the set point or the desired value of a variable in the system. From the adder, the error e(t) is calculated by subtracting measured system output x(t) from f(t). The calculated error is then passed to each of the components: integrator, differentiator, and constant multiplier. The values calculated parallelly from each component multiplied with the corresponding gain value are summed by an adder. The sum u(t) is the output from the PID controller, which also represents the calculated value that the actuator in the system needed to exert on a system. The general form of u(t) for a PID controller is

$$u(t) = K_p\, e(t) + K_i \int_0^t e(\tau)\, d\tau + K_d \frac{de(t)}{dt}, \quad (1)$$

where t is time, while K_p, K_i, and K_d are the proportional gain, the integral gain, and the derivative gain, respectively [18]. The three terms in the right-hand side of Equation (1) are calculated parallelly by the three mechanical components (integrator, differentiator, and constant multiplier). Therefore, by summing all three terms with an adder, the mechanical PID controller calculates Equation (1) for some given e(t).

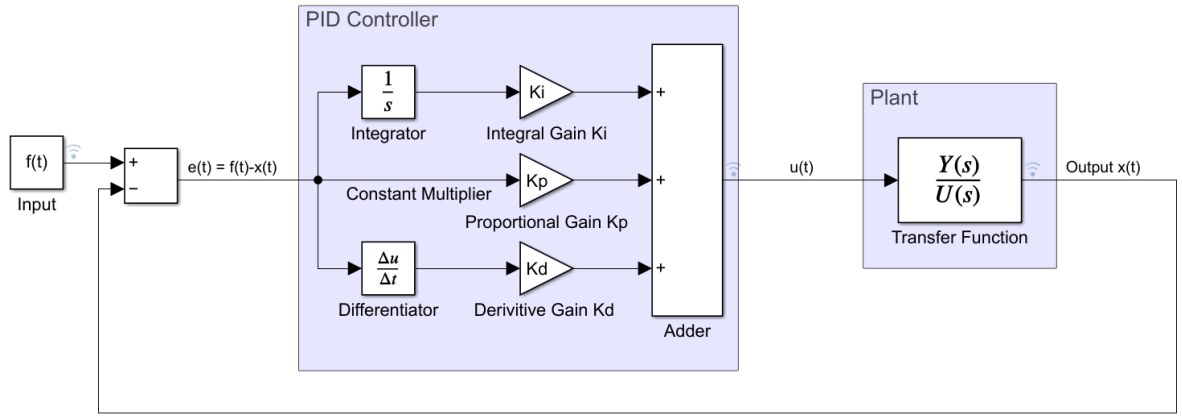

Fig. 1: A sample system with PID controller schematic in MATLAB.

3.2 Integrator

As shown in the above discussion, the realization of integral calculation is achieved by the integrator. An Omni-wheel-and-disk integrator is designed to calculate the integration of e(t). The design of the integrator follows V. Bush's wheel-and-disk design [8]. However, instead of using the Gonnella wheel, an Omni-wheel that bypasses the shaft-wise translation but transfers tangential movement into the shaft rotation is applied. As shown in Fig.2, the integrator integrates e(t) as a distance between the center of the disk and the wheel. It outputs the linear displacement of the rack spar $u_i(t)$ or the accumulated rotations of the main shaft. The disk is rotating at a constant angular velocity ω. Assuming no relative slip, when the Omni-wheel deviates from the center of the disk ($e(t)\neq 0$), the Omni-wheel will rotate at the same linear velocity of a circle with radius e(t) on the rotating disk. Then the gear will be driven by the Omni-wheel through the shaft. As the disk is continuously rotating, any input error e(t) other than zero will be accumulated over time. The output value u_i (t) from the integrator can be derived as follow

$$u_i(t)=\omega\frac{r_2}{r_1}\int_0^t e(\tau)\,d\tau=K_i\int_0^t e(\tau)\,d\tau \qquad e(\tau)\in(-R_{disk}, R_{disk}), \tag{2}$$

where K_i is a constant gain equal to $\omega\frac{r_2}{r_1}$.

Thus,

$$u_i(t)=K_i\int_0^t e(\tau)\,d\tau \qquad \text{for } e(\tau)\in(-R_{disk}, R_{disk}). \tag{3}$$

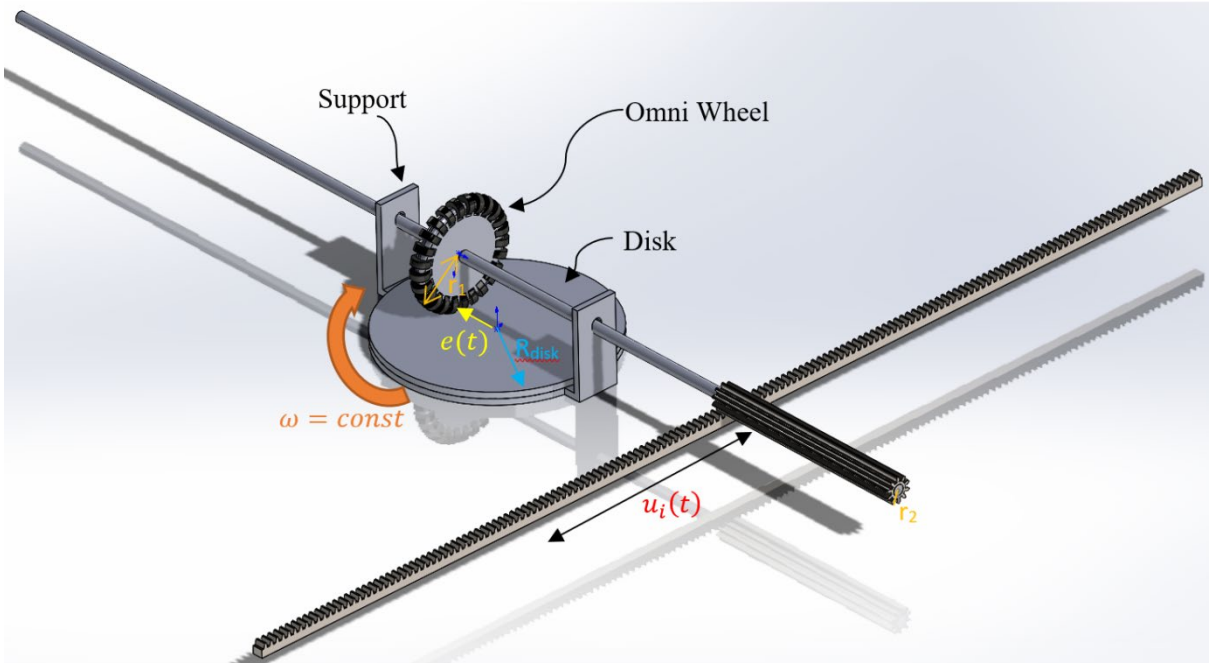

Fig. 2: The modeling of the mechanical integrator.

3.3 Differentiator

Similarly, the differentiator is aimed to calculate the differentiation of e(t). To order to characterize the effects of the new design of the mechanical differentiator, a physical model is established in this section (Fig. 3, Fig. 4). The differentiator is composed of the conveyor and a rotatable wheel connected to a cylindrical tangent cam. The conveyor operates at a constant linear velocity so that its upper surface moves at a constant speed v_x along the x-axis as shown in Fig. 3. Through the bevel gears, the rotation of the wheel along a vertical axis is converted to the rotation on the cam. The cylindrical tangent cam (Fig. 5) converts the rotation angle to the position of the pointer (pink in Fig. 3 and Fig. 4), which is also the corresponding tangent value. By moving the conveyor back and forth along the y-axis, e(t) can be input to the differentiator. Thus, the rate of change of error e'(t) is the velocity of the conveyor along the y-axis v_y. By contacting the wheel with the conveyor, the wheel tends to follow the moving direction of a point on the upper surface of the conveyor $\vec{v}=<v_x,v_y>=<v_x,e(t)>$. Thus, the angle of the wheel apart from the y axis, θ can be calculated

$$\theta = \tan^{-1}\left(\frac{v_y}{v_x}\right) = \tan^{-1}\left(\frac{e(t)}{v_x}\right), \theta \in \left(-\frac{\pi}{2}, \frac{\pi}{2}\right). \quad (4)$$

As mentioned above, the cylindrical cam (as presented in Fig. 5) is designed to calculate the tangent value of the corresponding angle. This is implemented by the slot shape with the function f_1 in cylindrical coordinate

$$f_1: (\rho, \varphi, z)=(R_{cam}, \theta, k\tan(\theta)), \theta \in \left(-\frac{\pi}{2}, \frac{\pi}{2}\right), \quad (5)$$

or in parametric equations

$$f_1: \begin{cases} x=R_{cam}\sin(\theta) \\ y=R_{cam}\cos(\theta) \\ z=k\tan(\theta) \end{cases}, \theta \in \left(-\frac{\pi}{2}, \frac{\pi}{2}\right). \quad (6)$$

where ρ is the radial distance from the z-axis, φ is the azimuth referenced from the yz-plane, z is the axial coordinate in z-axis, R_{cam} is the radius of the cam, θ is the rotation angle of the cam, and k is a scaling factor for better accuracy in calculation. Note that φ is equal to θ in this case because the bevel gears have gear ratio of 1:1.

In the modeling, the scaling factor k is chosen to be 3, which can then be easily canceled out by adding a mechanical constant multiplier (see Section 3.4) with a gain value equal to 1/3. Since tan(θ) diverges to infinity as θ approaches ±π/2, the limit here is set to (-1.51,1.51), which means the cam can calculate tan(θ) correctly for given θ in the range of (-86.51˚, 86.51˚). For θ outside of the range, the output is set to ±3tan(1.51), slightly smaller than half of the cam length h. Thus, in the range of (-1.51,1.51), the output $u_d(t)$ can be derived as follows

$$u_d(t)=z(\theta)=k\tan(\theta)=k\tan\left(\tan^{-1}\left(\frac{e(t)}{v_x}\right)\right)=\frac{k}{v_x}e(t) \quad \text{where } e(t)\in\left(-1.51\frac{v_x}{k},1.51\frac{v_x}{k}\right), \tag{7}$$

or

$$u_d(t)=K_d\, e(t),\ e(t)\in(-1.51/K_d,1.51/K_d), \tag{8}$$

where K_d is a constant gain equal to k/v_x. This indicates that the differentiator can calculate the derivative of e(t) in the given range!

Therefore, for all possible cases, the output from the differentiator can be described as

$$u_d(t)=\begin{cases} K_d\, e'(t), & e'(t)\in(-1.51/K_d,1.51/K_d) \\ k\ \tan(1.51), & e'(t)\in(1.51/K_d,\infty) \\ -k\tan(1.51), & e'(t)\in(-\infty,1.51/K_d) \end{cases} \quad for\ e\in\left(-\frac{L}{2},\frac{L}{2}\right) \tag{9}$$

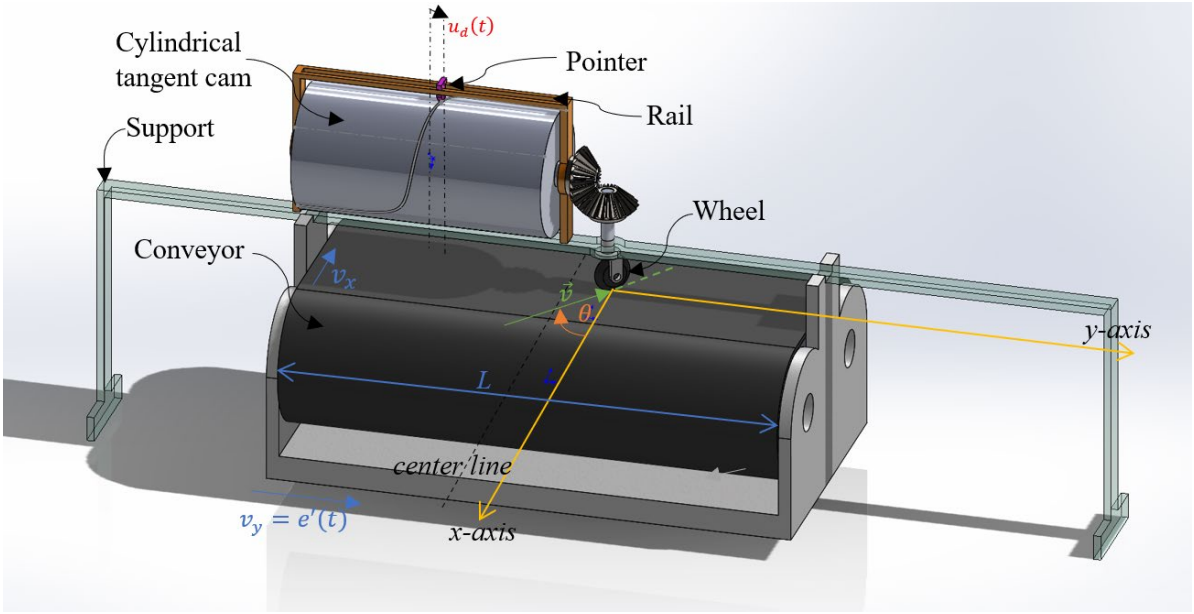

Fig. 3: The modeling of a mechanical differentiator. The indication of parts and the variables are also defined here.

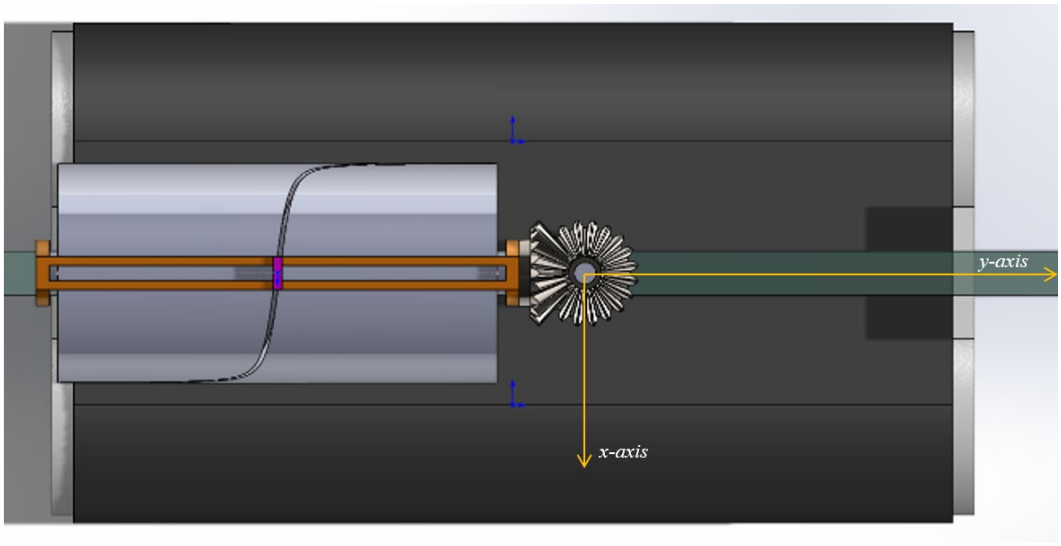

Fig. 4: The top view of the differentiator when the rotation angle θ is zero. In this case, the pointer is centered, and the cam outputs zero. (θ=0, ui (t)=0)

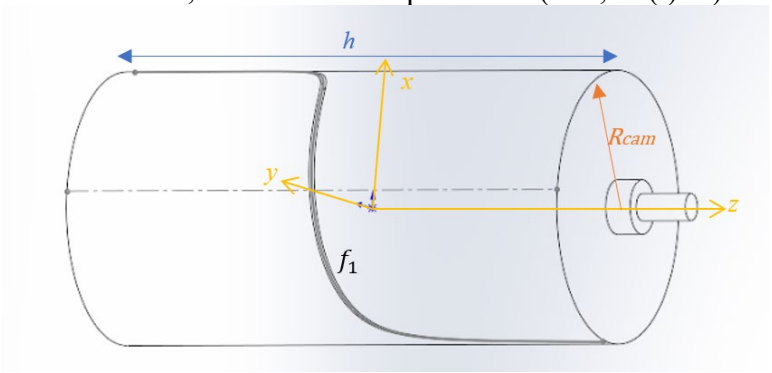

Fig. 5: The cylindrical tangent cam. Note that the x-y-z coordinate here is defined locally for the slot definition only.

3.4 Constant multiplier

The constant multiplier can be considered as a mechanical linear amplifier that multiplies the input value by a constant gain value. The gain K_p as shown in Equation 1 for the controller can be directly

calculated by concentric gears with different radius. e(t) is input to the device as a linear distance on the pitch circle of the inner gear. The output $u_p(t)$ is the linear distance on the pitch circle of the outer gear. Note that the two gears are fixed to each other, meaning there is no relative rotation between the two gears. The $u_p(t)$ can be derived as

$$u_p(t)=\frac{r_b}{r_a}e(t)=K_p\ e(t), \tag{10}$$

where r_a and r_b are radii of the pitch circle of the inner and outer circles and K_p is the proportional gain, or the gear ratio. Besides calculating the K_p, the constant multiplier can also be applied to the outputs from the integrator and differentiator to implement their gain values K_i and K_d.

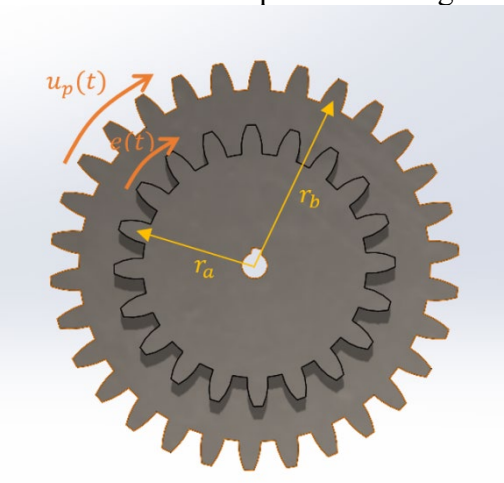

Fig. 6: The modeling of the constant multiplier.

3.5 Adder

As shown in the schematic (Fig. 1), adders sum the effect of each term in Equation 1. A mechanical differential is introduced to perform summation and substruction. For consistency, we call it an adder in the following description. As shown in Fig. 7, the adder has two inputs: rotations on Spur Gear 10 and Spur Gear 7. Note that Spur Gear 9 and Bevel Gear 10 are fixed to each other, and Spur gear 7 and Bevel Gear 8 are fixed to each other. Thus, the input rotation is then transferred to the rotation of Bevel Gear 1 and Bevel Gear 2, which can then be transferred to the rotation of the plus-shape center shaft 3. Except Spur Gear 6, all other gears on the center shaft can freely rotate around the shaft. The radius of Spur Gear 5, r is designed to have a half radius of other spur gears (Gear 4, 6, 7, and 10), R. (R=2r)

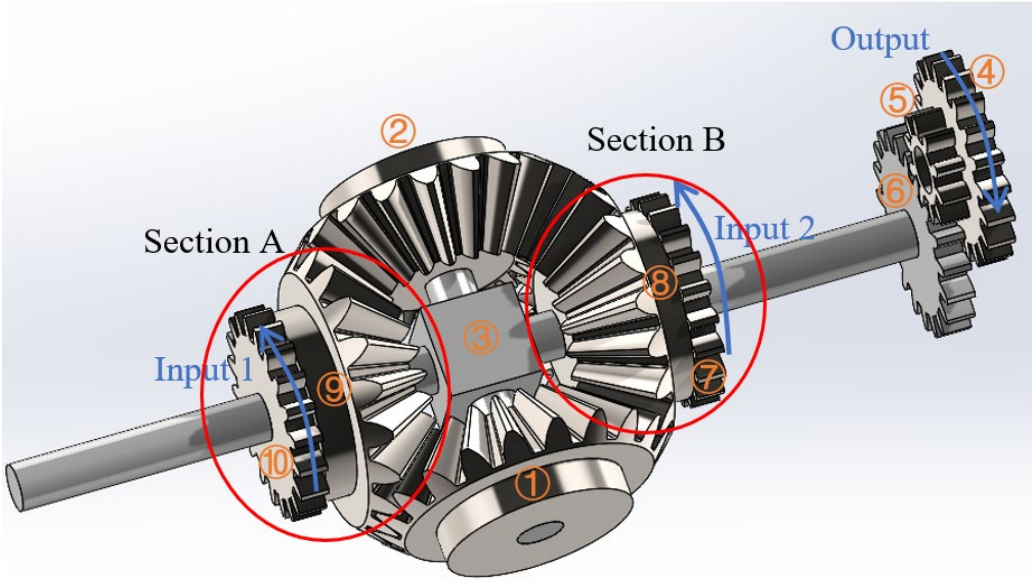

Fig. 7: The modeling of a mechanical adder. Components are indicated with serial numbers.

The rotation of the shaft θshaft can be derived as

$$\theta_{shaft}=\frac{\theta_1+\theta_2}{2}, \tag{11}$$

where θ_1 and θ_2 have rotated angles of Section A (Gear 9 and 10) and Section B (Gear 7 and 8) , respectively. The linear displacement of the pitch circle on Spur Gear 6, S_6 is

$$S_6=S_5=\theta_{shaft}\ R=\frac{\theta_1+\theta_2}{2}R=\frac{u_1+u_2}{2}, \tag{12}$$

where S_5 is the linear displacement of the pitch on Spur Gear 5, u_1 and u_2 are input linear displacement on Gear 10 and Gear 7 respectively. Then the output of the mechanical differential u_{out}, or the linear displacement on the Spur Gear 4 is

$$u_{out}=\frac{u_1+u_2}{2}*\frac{R}{r}=u_1+u_2\ (R=2r), \tag{13}$$

where R is the radius of Spur Gears 4, 6, 7, and 10, and r is the radius of Spur Sear 5.

Similarly, the mechanism can calculate three different inputs by connecting two adders as presented in Fig. 8 and Equation 14.

$$u_{out_{cascade}}=u_1+u_2+u_3 \tag{14}$$

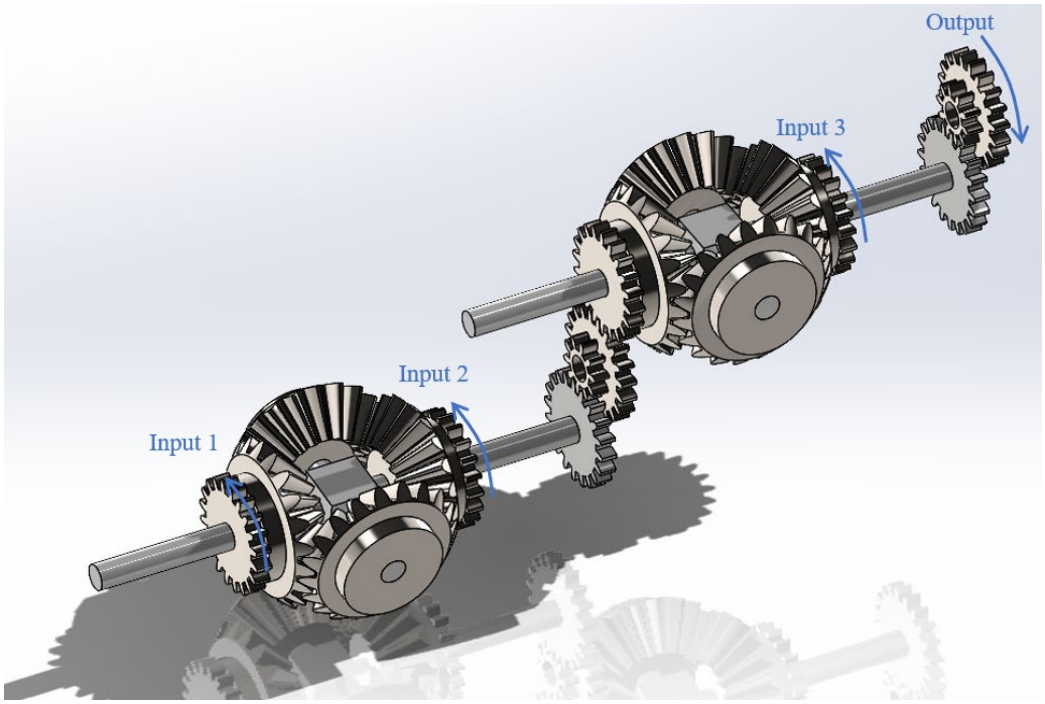

Fig. 8: The modeling of a two-stage cascaded adder that can add three inputs.

3.6 Synthesis

For the PID controller, the final output can be calculated by summing results from the integrator, differentiator, and linear amplifier using the cascaded adder in the pattern shown in Fig. 9. The output can then be applied back to the system for control purposes. The connection between components can be implemented with gears and spur racks. To ensure the mechanical PID controller functions in reality, additional devices including V. Bush's torque amplifier may be implemented between components [8].

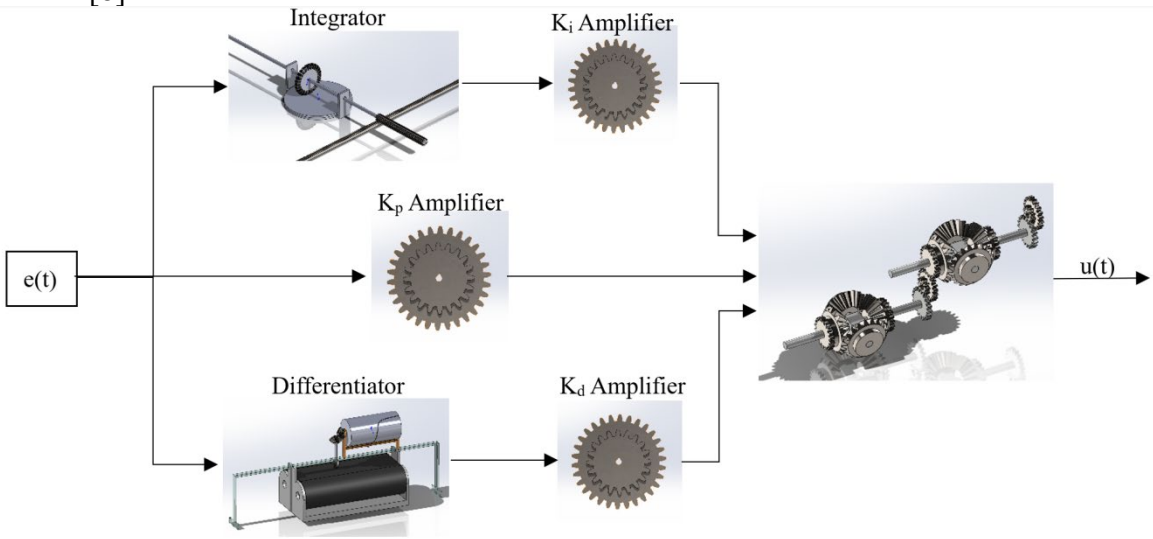

Fig. 9: The flow chart for mechanical PID controller (calculator).

4. Conclusion

The mechanical PID controller here borrows the idea of a mechanical analog computer. That is, instead of creating a dynamic system to obtain the feedback values u(t), the mechanical PID controller calculates the PID feedback by integration, differentiation, constant multiplication, and summation. From CAE modeling and mathematical derivation, the new form of PID control realization is proven to be functional in theory.

References

[1] S. Bennett, “The past of PID controllers,” Annu. Rev. Control, vol. 25, pp. 43–53, 2001, doi: 10.1016/S1367-5788(01)00005-0.

[2] J. T. Stock, “Pneumatic process controllers: The ancestry of the proportional-integral-derivative controller,” Trans. Newcom. Soc., vol. 59, no. 1, pp. 3–13, 1987, doi: 10.1179/tns.1987.003.

[3] S. Bennett, “Development of the PID controller,” IEEE Control Syst., vol. 13, no. 6, pp. 58–62, Dec. 1993, doi: 10.1109/37.248006.

[4] C. Erdal, A. Toker, and C. Acar, “A Proportional-Integral-Derivative (PID) Controller Realization by Using Current Feedback Amplifiers (CFAs) and Calculating Optimum Parameter Tolerances,” Journal of Applied Sciences, vol. 1, no. 3. pp. 325–328, 2001. doi: 10.3923/jas.2001.325.328.

[5] K. J. Åström and H. Steingrímsson, “Implementation of a PID Controller on a DSP,” 1990.

[6] J. Thomson, “III. On an integrating machine having a new kinematic principle,” Proc. R. Soc. London, vol. 24, no. 164–170, pp. 262–265, 1876, doi: 10.1098/rspl.1875.0033.

[7] P. S. W. Thomsom, “Mechanical Integration of the Linear Differntial Equations of the Second Order with Variable Coefficients,” in On Differential Equations of the Second Order, 1876, pp. 269–271.

[8] V. Bush, “The differential analyzer. A new machine for solving differential equations,” J. Franklin Inst., vol. 212, no. 4, pp. 447–488, 1931, doi: 10.1016/S0016-0032(31)90616-9.

[9] P. A. Holst, “Analog Computer,” in Encyclopedia of Computer Science, John Wiley and Sons Ltd., 2003, pp. 53–59. doi: 10.5555/1074100.

[10] J. R. Ragazzini, R. H. Randall, and F. A. Russell, “Analysis of Problems in Dynamics by Electronic Circuits,” Proc. IRE, vol. 35, no. 5, pp. 444–452, May 1947, doi: 10.1109/JRPROC.1947.232616.

[11] H. E. Criner, G. D. McCann, and C. E. Warren, “A New Device for the Solution of Transient-Vibration Problems by the Method of Electrical-Mechanical Analogy,” J. Appl. Mech., vol. 12, no. 3, pp. A135–A141, 1945, doi: 10.1115/1.4009454.

[12] G. . D. . McCann, “The California Institute of Technology Electric Analog Computer,” Am. Math. Soc., vol. 3, no. 28, pp. 501–513, 1949, doi: 10.1126/science.54.1389.119.

[13] J. E. Tomayko, “Helmut Hoelzer’s Fully Electronic Analog Computer,” Ann. Hist. Comput., vol. 7, no. 3, pp. 227–240, 1985, doi: 10.1109/MAHC.1985.10025.

[14] B. K. H. Lundberg, “The History of Analog Computing,” IEEE Control Systems Magazine, no. June, pp. 22–28, 2005.

[15] A. GOLDGAR, F. R. S. D. R. Hartree, and A. Porter, “Time-lag in a Control System,” Philos. Trans. R. Soc. LONDON, vol. 235, pp. 415–444, 1936, doi: 10.2307/j.ctt211qv60.7.

[16] S. Bennett, “A Brief History of Automatic Control,” IEEE Control Syst., vol. 16, no. 3, pp. 17–25, 1996, doi: 10.1109/37.506394.

[17] A. U. Keskin, “Design of a PID controller circuit employing CDBAs,” Int. J. Electr. Eng. Educ., vol. 43, no. 1, pp. 48–56, 2006, doi: 10.7227/IJEEE.43.1.5.

[18] B. Rooholahi and P. L. Reddy, “Concept and application of PID control and implementation of continuous PID controller in Siemens PLCs,” Indian J. Sci. Technol., vol. 8, no. 35, 2015, doi: 10.17485/ijst/2015/v8i35/82262.